Coexistence and interfacial properties of a triangle-well mimicking the Lennard-Jones fluid and a comparison with noble g....

Article *in* The Journal of Chemical Physics · February 2015

DOI: 10.1063/1.4909548 · Source: PubMed

5 authors, including:

Mariana Barcenas
Tecnologico de Estudios Superiores de Ecate...
15 PUBLICATIONS **108** CITATIONS
SEE PROFILE

Yuri Reyes-Mercado
45 PUBLICATIONS **495** CITATIONS
SEE PROFILE

Ascención Romero-Martínez
Instituto Mexicano del Petroleo
28 PUBLICATIONS **384** CITATIONS
SEE PROFILE

Gerardo Odriozola
Metropolitan Autonomous University
73 PUBLICATIONS **764** CITATIONS
SEE PROFILE

Coexistence and interfacial properties of a triangle-well mimicking the Lennard-Jones fluid and a comparison with noble gases

M. Bárcenas, Y. Reyes, A. Romero-Martínez, G. Odriozola, and P. Orea

Citation: The Journal of Chemical Physics **142**, 074706 (2015); doi: 10.1063/1.4909548
View online: http://dx.doi.org/10.1063/1.4909548
View Table of Contents: http://scitation.aip.org/content/aip/journal/jcp/142/7?ver=pdfcov
Published by the AIP Publishing

Coexistence and interfacial properties of a triangle-well mimicking the Lennard-Jones fluid and a comparison with noble gases

M. Bárcenas,[1] Y. Reyes,[2] A. Romero-Martínez,[3] G. Odriozola,[4] and P. Orea[4,a)]
[1]*División de Ingeniería Química y Bioquímica, Tecnológico de Estudios Superiores de Ecatepec (TESE), Av. Tecnológico S/N, 55210 Edo. de México, Mexico*
[2]*Departamento de Recursos de la Tierra, Universidad Autónoma Metropolitana Unidad Lerma (UAM-L), Av. Hidalgo Pte. 46, Col. La Estación, 52006 Lerma de Villada, Mexico*
[3]*Instituto Mexicano del Petróleo, Dirección de Investigación en Exploración y Producción, Eje Central Lázaro Cárdenas 152, 07730 México D.F., Mexico*
[4]*Instituto Mexicano del Petróleo, Dirección de Investigación en Transformación de Hidrocarburos, Eje Central Lázaro Cárdenas 152, 07730 México D.F., Mexico*

(Received 25 November 2014; accepted 6 February 2015; published online 20 February 2015)

Coexistence and interfacial properties of a triangle-well (TW) fluid are obtained with the aim of mimicking the Lennard-Jones (LJ) potential and approach the properties of noble gases. For this purpose, the scope of the TW is varied to match vapor-liquid densities and surface tension. Surface tension and coexistence curves of TW systems with different ranges were calculated with replica exchange Monte Carlo and compared to those data previously reported in the literature for truncated and shifted (STS), truncated (ST), and full Lennard-Jones (full-LJ) potentials. We observed that the scope of the TW potential must be increased to approach the STS, ST, and full-LJ properties. In spite of the simplicity of TW expression, a remarkable agreement is found. Furthermore, the variable scope of the TW allows for a good match of the experimental data of argon and xenon. © *2015 AIP Publishing LLC.* [http://dx.doi.org/10.1063/1.4909548]

I. INTRODUCTION

Calculating the thermodynamic properties of molecular systems from model potentials is one of the main aims of statistical mechanics. This has been done through simulation techniques as well as theoretical approaches. Since early works, pairwise additive potentials have been helpful to understand the experimental behavior and reproduce the thermodynamic properties of such systems. One of the most widely studied potentials has been the Lennard-Jones (LJ) because, while simple, it is based on physical arguments (Pauli repulsion and van der Waals attraction). Furthermore, it provides a reasonable fit to quantum calculations and produces accurate results for the thermodynamic properties of some neutral atoms such as noble gases.[1–8]

A drawback of the LJ pair potential when implemented in simulations is that it requires a certain treatment to correctly account for its long range tail.[9–12] These treatments usually make use of slab-based corrections,[10,13] Ewald summation techniques,[14] or simply avoid the issue by setting a very long cutoff radius which leads to long running times (the simulation time roughly scales with the cube of the cutoff assuming there is no other contribution to the potential). The diverse implementations vary their degree of complexity and yield results with different accuracies for a given computational cost. Indeed, the most frequent implementations make use of the so called spherically truncated and shifted (STS) and the spherically truncated (ST) Lennard Jones potentials, both truncated at 2.5 times the length at which the potential is zero, σ. The full-LJ, the STS, and the ST implementations differ from each other and hence produce different results. Also, there are many works where the Pauli repulsion and van der Waals attraction are modeled by using alternative pair potentials of easier handling to avoid the problem of the cutoff radius.[15–17]

In this paper, we further explore the above mentioned idea by means of the triangle well (TW) potential. This functional shape has been studied from the very beginning of computer simulations[15,18,19] to these days.[17,20,21] The TW has the advantage of having a simple mathematical shape which allows to easily deal with theoretical approaches.[20,22] Furthermore, and more importantly for our current purpose, it has the advantage of having no tail and so it allows for a transparent, easy, and computationally cheap implementation in Monte Carlo and molecular dynamic simulations.[21–24] That is, since there is no need of defining a cutoff radius, it naturally avoids the implementation of special treatments for long-range potentials.[9–12] As in the LJ potential, the TW has a parameter defining the particle size, σ, and another modulating the depth of the attraction, ϵ. In addition, the TW defines an extra parameter which tunes the attraction range, λ. This makes the TW more flexible than the LJ. Hence, there should be λ values which may approximate the TW thermodynamic properties to those corresponding to the several usual implementations of the LJ potential. Giving an answer to the question—how well these properties are reproduced?—is one of the aims of this work. The second would be to compare the thermodynamic properties of the TW fluid directly with experimental data. Again, the extra parameter defining the potential range aids to this purpose.

a)Author to whom correspondence should be addressed. Electronic mail: porea@imp.mx

Several simulation works have been focused on reproducing the thermodynamic properties of noble gases,[4,7,25–30] however, only a few were able to provide satisfactory results.[4,6,26,28–30] The difficulty lies on that potentials based on fittings to precise quantum mechanical data should take explicitly into account three body interactions. For instance, Goujon *et al.*[6] have performed this kind of simulations for the liquid-vapor interface of argon and conclude stating that "*Some 40 years after the first direct simulations of the surface tension of argon, we have achieved a reconciliation between the simulation and experiment by including the three-body interactions in the simulation*." Nonetheless, an effective pairwise potential may also roughly capture such contributions. In this work, we show that the TW potential can reasonably reproduce the coexistence and interface properties of argon and xenon, without the need of explicitly including three-body interactions as it has been done in several works yielding different outcomes.[3,4,26,28–30] For this purpose, we have fitted λ.

II. POTENTIAL MODEL AND SIMULATION METHOD

The TW potential is given by

$$U(x) = \begin{cases} \infty, & \text{for } x \le 1, \\ \epsilon(x-\lambda)/(\lambda-1), & \text{for } 1 < x \le \lambda, \\ 0, & \text{for } \lambda < x, \end{cases} \tag{1}$$

where $x = r/\sigma$ is the reduced distance, σ is the hard-core diameter, ϵ is its potential depth, and λ is the interaction range or scope ($\lambda > 1$).[15,21–23]

The surface tension results are calculated by using the virial route

$$\gamma = \frac{L_z}{2}\left\{\langle P_{zz}\rangle - \frac{1}{2}[\langle P_{xx}\rangle + \langle P_{yy}\rangle]\right\}, \tag{2}$$

where P_{ii} $(i = x, y, z)$ are the diagonal components of the pressure tensor and L_z is the length of the simulation box side which is normal to the interfaces. The factor 1/2 is due to the existence of two interfaces inside the cell. This route is allowed by implementing the extrapolation procedure given in detail in previous works[9,21,31] to deal with discontinuities.

Results are given in dimensionless units as follows: $T^* = k_B T/\epsilon$ for temperature (being k_B the Boltzmann constant), $\rho^* = \rho\sigma^3$ for number density, and $\gamma^* = \gamma\sigma^2/\epsilon$ for surface tension. The critical density and temperature are calculated by using the rectilinear diameters law and the universal exponent $\beta = 0.325$.[32,33]

Simulations were carried out in the vapor-liquid region and performed in parallelepiped boxes with sides $L_x = L_y = 10\sigma$ and $L_z = 4 \times L_x$. Periodic boundary conditions are considered in the three directions. Each cell is initially set with all particles ($N = 1200$), randomly placed within the liquid slab, and surrounded by vacuum. The center of mass is placed at the box center and kept fixed there along cycles. Particles are moved by using the Metropolis algorithm and Verlet-lists are employed to speed up calculations.[32,33] The highest temperature (T^*_{max}) was set close to and below the critical temperature of the system, while the other temperatures are established by following a decreasing geometric progression, i.e., $T^*_i = T^*_{max}(T^*_{min}/T^*_{max})^{(i-1)/(M-1)}$, where T^*_{min} is the lowest temperature and M is the number of state points. Maximum displacements are varied to yield acceptance rates close to 30%. We combine the slab technique[34] with the replica exchange method.[32,33,35–37] The M replicas are equilibrated by 10^7 steps. The results reported in this work are calculated by analyzing additional 4×10^7 steps, as it has been done in previous works.[21,31]

As mentioned, simulations are carried out by using the replica exchange Monte Carlo (REMC) method which improves sampling at low temperatures. The implementation of the expanded ensemble involves conducting standard MC canonical simulations at each replica with the additional step of considering trial moves that attempt to swap the replicas from one ensemble to another. The introduction of swap trials makes a particular replica to travel through many temperatures allowing it to overcome free energy barriers. So, M ensembles are simultaneously considered, each one with a different temperature. Replicas at high temperatures travel long distances in configuration space, whereas low temperature replicas perform precise sampling at local regions of configuration space.

Swaps are based on the definition of an extended ensemble whose partition function reads

$$Q_{ext} = \prod_{i=1}^{M} Q_{NVT^*_i}, \tag{3}$$

where $Q_{NVT^*_i}$ is the partition function of the canonical ensemble of the system at temperature T^*_i, volume V, with N particles. We set the number of replicas equal to the number of ensembles M.

To fulfill detailed balance, the acceptance probability for swap trials is given by

$$P_{acc} = min(1, \exp[(\beta_j - \beta_i)(U_i - U_j)]), \tag{4}$$

where $U_i - U_j$ is the potential energy difference between replicas i and j, and $\beta_i - \beta_j$ is the difference between the reciprocal temperatures ($\beta_i \equiv 1/(k_B T_i)$). Adjacent temperatures should be close enough to provide large exchange acceptance rates between neighboring ensembles.

III. RESULTS AND DISCUSSION

In this section, we present computer simulation results for the coexistence and interfacial properties of an attractive TW fluid with different ranges. The section is split into two parts. In Subsection III A, the obtained results are compared to the corresponding simulation data of the LJ potential. In the next, the TW results are compared to experimental data of argon and xenon.

A. TW vs LJ fluids

As mentioned in the Introduction, several alternatives to the well-known LJ potential have been attempted to avoid the long tail issue.[15–17] To the best of our knowledge, the TW has not been tried yet. In this section, we compare the TW coexistence and interfacial properties with those corresponding to the different implementations of the LJ for several λ values. The

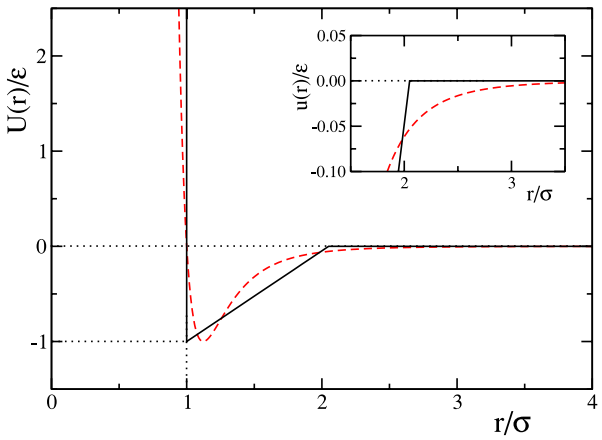

FIG. 1. Lennard-Jones (red dashed line) compared to the TW with λ = 2.05 (black solid line). The inset zooms in the tail region. Both potentials produce similar thermodynamic properties.

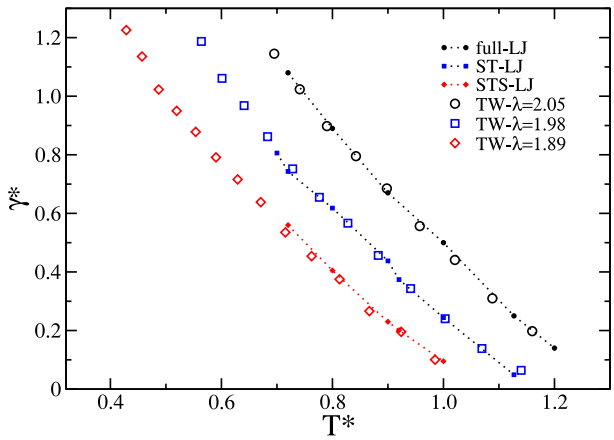

FIG. 3. Comparison of the surface tension for the different implementations of the LJ and the TW models with different λ values. The data are in correspondence with those given in Fig. 2. Here, the agreement is remarkable.

idea is to evaluate how well the TW mimics the LJ fluid. For this purpose, we have matched the hard-core diameter of the triangle well fluid, σ, to the distance at which the LJ potential crosses zero (see Figure 1).

Fig. 2 shows the coexistence phase diagrams of TW fluids having three different ranges: λ = 1.89, 1.98, and λ = 2.05. It also includes the simulation data reported in the literature for different implementations of the LJ potential for a direct comparison.[9] These different implementations are the ST, the STS, and the full-LJ. Both, the ST and STS are set by considering a cutoff radius of 2.5σ. There are, however, other cutoff distances available in the literature (see Refs. 8, 11, 13, and 38). For a cutoff distance above 6.5σ, the outcomes from all variants of the LJ potential are essentially the same.[39] On the other hand, the full-LJ is obtained by making use of Ewald summations[14] (note that other simpler treatments are also available[6]). The three different implementations of the LJ potential produce clearly different coexistence curves. Consequently, the TW range λ must be increased to follow the series STS, ST, and full-LJ. This is expected since the long tail contribution is absent for the STS and ST, and besides the STS has a shallower minimum (it is shifted upwards to avoid the discontinuity at the cutoff). We have tried several λ values, and the best matches (considering both the coexistence densities and surface tension) are the ones we are presenting. The matching among the vapor branches is very good for the three cases. The liquid densities are not in excellent agreement, though. Systematically, the TW liquid densities are lower than the LJ-type which is close to the critical point and crosses through larger densities as the temperature is decreased. This is related to the different locations of the minimum of the potential (see Fig. 1). Lowering the temperature produces configurations with an average inter-particle distance closer to the potential minimum, which is smaller for the TW. Hence, the liquid density of the TW turns larger than that of the LJ liquid for the three cases.

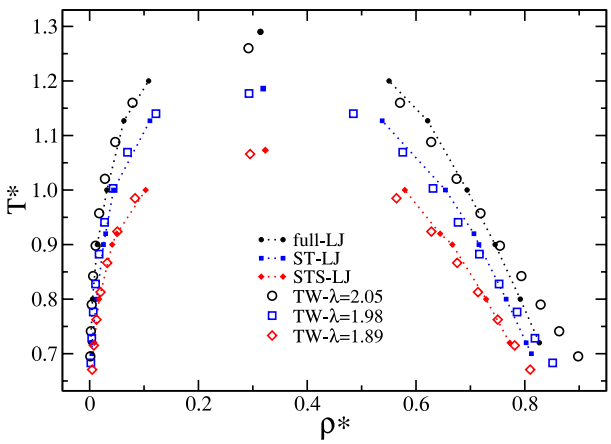

FIG. 2. Comparison of the coexistence densities of the different implementations of the LJ potential with the properties of the TW model with different λ values. The STS, ST, and full-LJ roughly correspond to TW fluids with λ = 1.89, 1.98, and 2.05, respectively.

Fig. 3 shows the surface tension curves corresponding to the liquid-vapor phase diagrams shown in Fig. 2. As for the coexistence densities, the surface tension values for the three implementations of the LJ strongly differ. Larger surface tension values are obtained as changing from STS, ST to full-LJ implementations. Hence, the order of the series is kept invariant. The matching of the TW data to the LJ surface tension values produces excellent agreements. This is so despite the slight mismatch found between the densities of the liquid branches. We should also point out the clearer trends obtained for the TW, which expands towards lower temperatures than those previously reported for the LJ fluids.

Finally, in Fig. 4, we show the comparison of the surface tension of a full-LJ fluid calculated by different techniques. Each of these techniques was employed with the aim of precisely calculating the surface tension of this long-range potential. As can be observed, the TW potential with λ = 2.05 reproduces correctly the full LJ data. This is done without the need of implementing treatments for handling the long range tail. Naively, one would not expect a tailless potential to reproduce the surface tension of a long-range potential.

B. TW vs noble gases

As mentioned in the Introduction, reproducing the thermodynamic properties of molecular systems from model

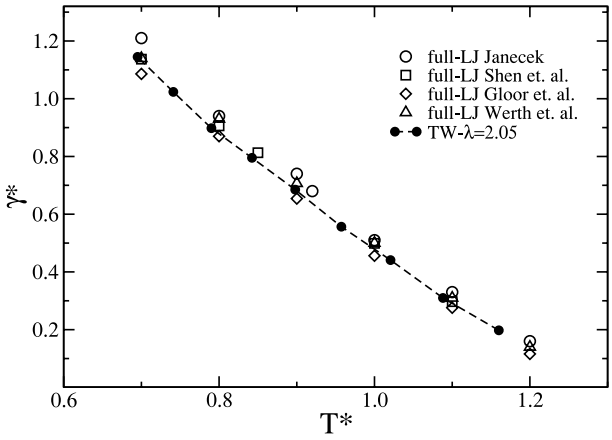

FIG. 4. Surface tension of full LJ fluid from different authors[10,11,14,40,41] and by employing different simulation techniques (open symbols). We are also including the TW data obtained for $\lambda = 2.05$ as solid symbols. The TW mimics the full LJ fluid despite being tailless.

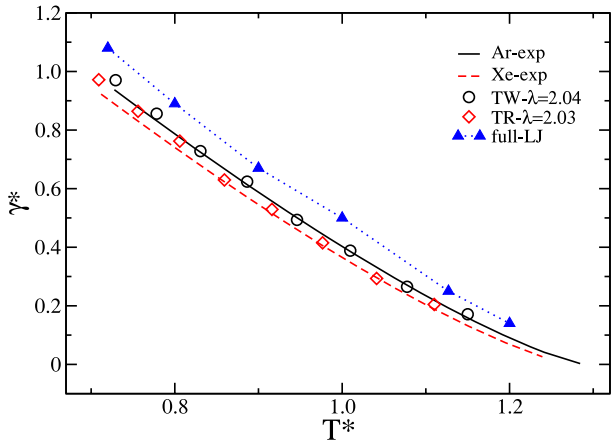

FIG. 6. Comparison of the surface tension of argon and xenon with the TW model for $\lambda = 2.04$ and 2.03, respectively. Full-LJ are also shown as solid symbols.[14] All data are in correspondence with those given in Fig. 5. Experimental data are taken from Ref. 42 and normalized by considering $\epsilon/k_B = 116.79$ K, $\sigma = 3.3952$ A and $\epsilon/k_B = 227.55$ K, $\sigma = 3.9011$ A for argon and xenon, respectively.[2]

potentials has been one of the main goals of simulations. Contrasting with the LJ case, the TW potential has not been directly considered for this purpose. In this section, we compare the TW coexistence and interfacial properties to those of argon and xenon. In the literature, the LJ potential is accepted as a good model for these two noble gases.

Fig. 5 shows the normalized coexistence data for both, argon and xenon, and those obtained with the TW potential for $\lambda = 2.04$ and 2.03. We have also included the results obtained with the full LJ potential. As can be seen, the full LJ potential excellently matches the argon coexistence densities. The xenon liquid branch is slightly shifted to smaller densities than that of argon, and so the LJ liquid branch also deviates from it. The trends of both branches, liquid and vapor, very well agree between experiments and the LJ data. Nonetheless, this is not true for the interfacial properties as we discuss in the following paragraph. On the other hand, the TW results for cases $\lambda = 2.04$ and 2.03 approach argon and xenon experimental data, though

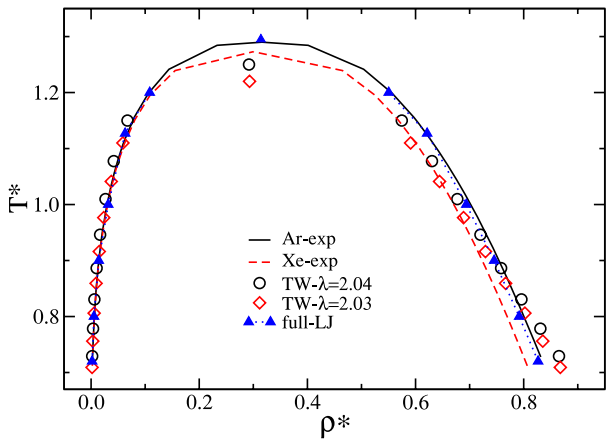

FIG. 5. Comparison of the coexistence densities of argon and xenon (lines) to the corresponding properties of the TW potential with $\lambda = 2.045$ and 2.030 (open symbols). LJ data are also included as solid symbols.[14] Experimental data are taken from Ref. 42 and reduced by considering $\epsilon/k_B = 116.79$ K, $\sigma = 3.3952$ A and $\epsilon/k_B = 227.55$ K, $\sigma = 3.9011$ A for argon and xenon, respectively.[2]

the agreement is not the best for the liquid region. This is in line with the observations made in Sec. III A.

In Fig. 6, we show the comparison of experimental surface tension data for argon and xenon with the simulation results for the TW potential with $\lambda = 2.04$ and 2.03. As can be seen, the agreement is remarkable. This is so, even despite the fact that the agreement for the coexistence is not excellent. On the other hand, the full-LJ data clearly overestimate the experimental data for the considered temperature range. Recently, an implementation of the three body contribution of the full-LJ has been able to reproduce the experimental surface tension of argon while keeping the correctness of the coexistence densities.[6] Implementing three body contributions is somewhat intricate and computationally expensive, though. Our simulation results were obtained with a simple implementation of a pairwise additive potential. Furthermore, the short range allows for small neighbor lists, which dictates the efficiency of the simulations, i.e., the simulation time roughly scales with the cube of the cutoff. When comparing the full-LJ (cutoff of 6σ when implemented directly) with the TW with $\lambda = 2.05$, the gain exceeds a factor of ten. The obtained results show that an effective pairwise additive TW potential can correctly predict the coexistence and interfacial properties of argon and xenon, by somehow compensating the long tail of the interparticle potential, inherent of molecules.

IV. CONCLUSIONS

Vapor-liquid coexistence densities and interfacial tensions of hard-core attractive triangle-well systems were calculated by using replica exchange Monte Carlo simulations. We observed that the fluids with $\lambda = 1.89, 1.98$, and 2.05 are suitable for mimicking truncated and shifted, truncated (both with a 2.5σ cutoff distance), and full Lennard Jones fluids, respectively. Aside from small quantitative differences, the reported coexistence data show an overall good agreement with the three types of Lennard-Jones fluids. We highlight that the

triangle-well potential does not have a tail extending through space, which allows for small Verlet lists and avoids long range special treatments. In other words, its computational cost is many times cheaper.

The variable scope of the triangle-well potential allows fitting experimental data. This way we have been able to reproduce the coexistence and interfacial properties of argon and xenon. The agreement found between the obtained and experimental properties is very good, despite the absence of long tail of the triangle-well model. From this comparison, we can conclude that this effective potential is a valid alternative to calculate the vapor-liquid coexistence densities and interfacial tension of molecules with spherical symmetry, probably due to a fortuitous cancellation of errors which compensates the long range interaction inherent of molecules. Moreover, any type of complex molecule, such as proteins, lipids, or asphaltanes, can eventually be modeled by means of an all-atom empirical force fields based on a triangle-well description. This would shorten the long running times of such large systems.

ACKNOWLEDGMENTS

G.O., A.R.M., and P.O. thank The Instituto Mexicano del Petróleo for financial support (Project Nos. D.60019 and 169125). M.B. thanks TESE. All the authors acknowledge the support of CONACyT.

[1]J. k. Lee, J. A. Barker, and G. M. Pound, J. Chem. Phys. **60**, 1976 (1974).
[2]J. Vrabec, J. Stoll, and H. Hasse, J. Phys. Chem. B **105**, 12126 (2001).
[3]J. A. Anta, E. Lomba, and M. Lombardero, Phys. Rev. E **55**, 2707 (1997).
[4]K. Leonhard and U. K. Deiters, Mol. Phys. **98**, 1603 (2000).
[5]K. Binder, Mol. Phys. **108**, 1797 (2010).
[6]F. Goujon, P. Malfreyt, and D. J. Tildesley, J. Chem. Phys. **140**, 244710 (2014).
[7]E. A. Ustinov and D. D. Do, J. Colloid Interface Sci. **366**, 216 (2012).
[8]D. O. Dunikov, S. P. Malyshenko, and V. V. Zhakhovskii, J. Chem. Phys. **115**, 6623 (2001).
[9]A. Trokhymchuk and J. Alejandre, J. Chem. Phys. **111**, 8510 (1999).
[10]J. Janecek, J. Phys. Chem. B **110**, 6264 (2006).
[11]V. K. Shen, R. D. Mountain, and J. R. Errington, J. Phys. Chem. B **111**, 6198 (2007).
[12]S. Werth, G. Rutkai, J. Vrabec, M. Horsch, and H. Hasse, Mol. Phys. **112**, 2227 (2014).
[13]M. Mecke, J. Winkelmann, and J. Fischer, J. Chem. Phys. **107**, 9264 (1997).
[14]J. López-Lemus and J. Alejandre, Mol. Phys. **100**, 2983 (2002).
[15]M. J. Feinberg and A. G. De Rocco, J. Chem. Phys. **41**, 3439 (1964).
[16]Y. Tang, Z. Tong, and B. C.-Y. Lu, Fluid Phase Equilib. **134**, 21 (1997).
[17]J. Krejci, I. Nezbeda, R. Melnyk, and A. Trokhymchuk, Condens. Matter Phys. **14**, 33005 (2011).
[18]T. Nagamiya, Proc. Phys.-Math. Soc. Jpn. **22**, 705 (1940).
[19]P. C. Wankhede and K. N. Swamy, Can. J. Phys. **55**, 632 (1977).
[20]L. D. Rivera, M. Robles, and M. López de Haro, Mol. Phys. **110**, 1317 (2012).
[21]M. Bárcenas, G. Odriozola, and P. Orea, Mol. Phys. **112**, 2114 (2014).
[22]F. F. Betancourt-Cárdenas, L. A. Galicia-Luna, A. L. Benavides, J. A. Ramírez, and E. Schöll-Paschinger, Mol. Phys. **106**, 113 (2008).
[23]J. Adhikari and D. A. Kofke, Mol. Phys. **100**, 1543 (2002).
[24]P. Orea and G. Odriozola, J. Chem. Phys. **138**, 214105 (2013).
[25]R. J. Sadus and J. M. Prausnitz, J. Chem. Phys. **104**, 4784 (1996).
[26]G. Marcelli and R. J. Sadus, J. Chem. Phys. **111**, 1533 (1999).
[27]D. Zhou, M. Zeng, J. Mi, and C. Zhong, J. Phys. Chem. B **115**, 57 (2011).
[28]E. K. Goharshadi and M. Abbaspour, J. Chem. Theory Comput. **2**, 920 (2006).
[29]W. Cencek, G. Garberoglio, A. H. Harvey, M. O. McLinden, and K. Szalewicz, J. Phys. Chem. A **117**, 7542 (2013).
[30]F. del Río, E. Díaz-Herrera, O. Guzmán, J. A. Moreno-Razo, and J. E. Ramos, J. Chem. Phys. **139**, 184503 (2013).
[31]G. Odriozola, M. Bárcenas, and P. Orea, J. Chem. Phys. **134**, 154702 (2011).
[32]D. Frenkel and B. Smit, *Understanding Molecular Simulation* (Academic, New York, 1996).
[33]M. P. Allen and D. J. Tildesley, *Computer Simulation of Liquids* (Clarendon, Oxford, 1986).
[34]G. A. Chapela, G. Saville, S. M. Thompson, and J. S. Rowlinson, J. Chem. Soc. Faraday Trans. II **73**, 1133 (1977).
[35]A. P. Lyubartsev, A. A. Martsinovski, S. V. Shevkunov, and P. N. Vorontsov-Velyaminov, J. Chem. Phys. **96**, 1776 (1992).
[36]E. Marinari and G. Parisi, Europhys. Lett. **19**, 451 (1992).
[37]K. Hukushima and K. Nemoto, J. Phys. Soc. Jpn. **65**, 1604 (1996).
[38]P. Grosfils and J. F. Lutsko, J. Chem. Phys. **130**, 054703 (2009).
[39]A. Ahmed and R. J. Sadus, J. Chem. Phys. **131**, 174504 (2009).
[40]G. J. Gloor, G. Jackson, F. J. Blas, and E. de Miguel, J. Chem. Phys. **123**, 134703 (2005).
[41]S. Werth, S. V. Lishchuk, M. Horsch, and H. Hasse, Physica A **392**, 2359 (2013).
[42]N. B. Vargaftik, *Handbook of Physical Properties of Liquids and Gases: Pure Substances and Mixtures*, 2nd ed. (Washington: Hemisphere, Washington, DC, 1975).